THE JOURNAL OF BIOLOGICAL CHEMISTRY VOL. 284, NO. 29, pp. 19402–19411, July 17, 2009
Printed in the U.S.A.

Structural Determinants of G-protein α Subunit Selectivity by Regulator of G-protein Signaling 2 (RGS2)*[S]

Received for publication, February 27, 2009, and in revised form, May 24, 2009 Published, JBC Papers in Press, May 28, 2009, DOI 10.1074/jbc.M109.024711

Adam J. Kimple[‡], Meera Soundararajan[§], Stephanie Q. Hutsell[¶], Annette K. Roos[§], Daniel J. Urban[‡], Vincent Setola[‡‖], Brenda R. S. Temple[¶], Bryan L. Roth[‡‖], Stefan Knapp[§‡‡], Francis S. Willard[‡1,2], and David P. Siderovski[‡§§1,3]**

*From the Departments of [‡]Pharmacology and [¶]Biochemistry and Biophysics, [‖]National Institute of Mental Health Psychoactive Drug Screening Program, [§§]Lineberger Comprehensive Cancer Center, and **R.L. Juliano Structural Bioinformatics Core Facility, University of North Carolina, Chapel Hill, North Carolina 27599 and the [§]Structural Genomics Consortium and [‡‡]Department of Clinical Pharmacology, Oxford University, Oxford OX3 7DQ, United Kingdom*

"Regulator of G-protein signaling" (RGS) proteins facilitate the termination of G protein-coupled receptor (GPCR) signaling via their ability to increase the intrinsic GTP hydrolysis rate of Gα subunits (known as GTPase-accelerating protein or "GAP" activity). RGS2 is unique in its *in vitro* potency and selectivity as a GAP for Gα_q subunits. As many vasoconstrictive hormones signal via G_q heterotrimer-coupled receptors, it is perhaps not surprising that RGS2-deficient mice exhibit constitutive hypertension. However, to date the particular structural features within RGS2 determining its selectivity for Gα_q over G$\alpha_{i/o}$ substrates have not been completely characterized. Here, we examine a trio of point mutations to RGS2 that elicits Gα_i-directed binding and GAP activities without perturbing its association with Gα_q. Using x-ray crystallography, we determined a model of the triple mutant RGS2 in complex with a transition state mimetic form of Gα_i at 2.8-Å resolution. Structural comparison with unliganded, wild type RGS2 and of other RGS domain/Gα complexes highlighted the roles of these residues in wild type RGS2 that weaken Gα_i subunit association. Moreover, these three amino acids are seen to be evolutionarily conserved among organisms with modern cardiovascular systems, suggesting that RGS2 arose from the R4-subfamily of RGS proteins to have specialized activity as a potent and selective Gα_q GAP that modulates cardiovascular function.

G protein-coupled receptors (GPCRs)[4] form an interface between extracellular and intracellular physiology, as they convert hormonal signals into changes in intracellular metabolism and ultimately cell phenotype and function (1–3). GPCRs are coupled to their underlying second messenger systems by heterotrimeric guanine nucleotide-binding protein ("G-proteins") composed of three subunits: Gα, Gβ, and Gγ. Four general classes of Gα subunits have been defined based on functional couplings (in the GTP-bound state) to various effector proteins. G_s subfamily Gα subunits are stimulatory to membrane-bound adenylyl cyclases that generate the second messenger 3′,5′-cyclic adenosine monophosphate (cAMP); conversely, G_i subfamily Gα subunits are generally inhibitory to adenylyl cyclases (4). $G_{12/13}$ subfamily Gα subunits activate the small G-protein RhoA through stimulation of the GEF subfamily of RGS proteins, namely p115-RhoGEF, LARG, and PDZ-RhoGEF (5). G_q subfamily Gα subunits are potent activators of phospholipase-Cβ enzymes that generate the second messengers diacylglycerol and inositol triphosphate (6); more recently, two additional Gα_q effector proteins have been described: the receptor kinase GRK2 and the RhoA nucleotide exchange factor p63RhoGEF (7, 8).

The duration of GPCR signaling is controlled by the time Gα remains bound to GTP before its hydrolysis to GDP. RGS proteins are key modulators of GPCR signaling by virtue of their ability to accelerate the intrinsic GTP hydrolysis activity of Gα subunits (reviewed in Refs. 9 and 10). RGS2/G0S8, one of the first mammalian RGS proteins identified (11) and member of the R4-subfamily (10), has a critical role in the maintenance of normostatic blood pressure both in mouse models (12, 13) and in humans (14, 15); additionally, *Rgs2*-deficient mice exhibit impaired aggression and increased anxiety (16, 17), behavioral phenotypes with potential human clinical correlates (18, 19).

Although many RGS proteins are promiscuous and thus act on multiple Gα substrates *in vitro* (*e.g.* Ref. 20), RGS2 exhibits exquisite specificity for Gα_q in biochemical binding assays and single turnover GTPase acceleration assays (20, 21). Consistent with this *in vitro* selectivity,[5] mice deficient in RGS2 uniquely exhibit constitutive hypertension and prolonged responses to

* This work was supported, in whole or in part, by National Institutes of Health Grants R01 GM082892 (to D. P. S.), T32 GM008570 (to S. Q. H.), and T32 GM008719 and F30 MH074266 (to A. J. K.). This work was also supported by American Heart Association Mid-Atlantic Affiliate Grant 0815239E (to D. J. U.).

[S] The on-line version of this article (available at http://www.jbc.org) contains supplemental Figs. S1–S3 and Tables S1 and S2.

The atomic coordinates and structure factors (code 2V4Z) have been deposited in the Protein Data Bank, Research Collaboratory for Structural Bioinformatics, Rutgers University, New Brunswick, NJ (http://www.rcsb.org/).

[1] Co-senior authors who contributed equally to this work.

[2] Present address: Lilly Research Laboratories, Eli Lilly and Company, Indianapolis, IN 46285.

[3] To whom correspondence should be addressed: 4073 Genetic Medicine Bldg., CB 7365, Chapel Hill, NC 27599. Tel.: 919-843-9363; Fax: 919-966-5640; E-mail: dsiderov@med.unc.edu.

[4] The abbreviations used are: GPCR, G-protein coupled receptor; FRET, Förster resonance energy transfer; RGS, regulator of G-protein signaling; SPR, surface plasmon resonance; YFP, yellow fluorescent protein; CFP, cyan fluorescent protein; PDB, Protein Data Bank; HA, hemagglutinin; CI, confidence interval; GTPγS, guanosine 5′-3-*O*-(thio)triphosphate; GAP, GTPase-accelerating protein.

[5] Independent reports (*e.g.*, Refs. 57–59) have demonstrated that, in membrane-reconstitution systems containing GPCRs and G-protein heterotrimers, RGS2 can affect the agonist-dependent GTPase activity of G_i-coupled signaling systems. The basis for this discrepancy between RGS2 selectivity for Gα_q in binary, solution-based assays and apparent RGS2 activity on Gα_i in reconstituted systems has not yet been resolved, but it is important to note that RGS2 (like other RGS proteins) is known to interact with other components of GPCR signal transduction beyond Gα subunits (60), including isoforms of the Gα_i effector target, adenylyl cyclase (37).

vasoconstrictors, as would be expected upon loss of a potent negative regulator of $G\alpha_q$ that mediates signaling from various vasoconstrictive hormones such as angiotensin II, endothelin, thrombin, norepinephrine, and vasopressin (22). In addition, RGS2-deficient mice respond to sustained pressure overload with an accelerated time course of maladaptive cardiac remodeling (23), a pathophysiological response that evokes myocardial hypertrophy known to be critically dependent on $G\alpha_q$ signaling (24, 25).

To gain insight into the structural basis of the unique $G\alpha$ substrate selectivity exhibited by RGS2, a series of point mutants in RGS2 were evaluated that enable this protein to bind and accelerate GTP hydrolysis by $G\alpha_i$; we subsequently delineated the structural determinants of the $G\alpha_i$/mutant RGS2 interaction using x-ray crystallography. Three key positions, first identified by Heximer and colleagues (21) and highlighted in our structural studies as key determinants of RGS2 substrate selection, were also found to be conserved throughout the evolution of the RGS2 protein in a manner suggestive of specialization toward cardiovascular signaling modulation.

EXPERIMENTAL PROCEDURES

Chemicals and Assay Materials—Unless otherwise noted, all chemicals were the highest grade available from Sigma or Fisher Scientific (Pittsburgh, PA).

Protein Expression and Purification—Using ligation-independent cloning, DNA encoding human RGS2 (Lys^{71}–His^{209}), fused to either hexahistidine alone (His_6) or to His_6-tagged enhanced yellow fluorescent protein (YFP), was hybridized into a Novagen (San Diego, CA) pET vector-based prokaryotic expression construct as previously described (26, 27). Point mutations corresponding to Cys^{106} to serine (C106S), Asn^{184} to aspartate (N184D), Arg^{188} to glutamate (R188E), and Glu^{191} to lysine (E191K) were made using QuikChange site-directed mutagenesis (Stratagene, La Jolla, CA). For expression of hexahistidine- and His_6-YFP fusion RGS2 constructs, BL21(DE3) *Escherichia coli* were grown to an $A_{600\ nm}$ of 0.7–0.8 at 37 °C before induction with 0.5 mM isopropyl β-D-thiogalactopyranoside. After culturing for 14–16 h at 20 °C, cells were pelleted by centrifugation and frozen at −80 °C. Bacterial pellets were then resuspended in N1 buffer (50 mM HEPES, pH 8.0, 400 mM NaCl, 30 mM imidazole, 5% (w/v) glycerol) and lysis of bacterial slurry was performed using an Emulsiflex (Avestin, Ottawa, Canada) according to the manufacturer's instructions. Cellular lysates were clarified by centrifugation at 100,000 × *g* for 30 min at 4 °C. The supernatant was applied to a Ni^{2+} chelating fast protein liquid chromatography column (FF HisTrap; GE Healthcare, Piscataway, NJ), washed with 7 column volumes of N1 buffer then 3 column volumes of N1 buffer containing an additional 30 mM imidazole before elution of recombinant RGS2 protein with N1 buffer containing 300 mM imidazole. His_6-tagged RGS2 protein was cleaved with tobacco etch virus protease overnight at 4 °C and dialyzed into N1 buffer containing 5 mM dithiothreitol. To separate residual His_6-RGS2 from untagged, cleaved RGS2, the protein was passed over a second Ni^{2+}-chelating fast protein liquid chromatography column. The flow-through was pooled, concentrated to final volume of ~5 ml, and resolved using a calibrated 150-ml size exclusion column (Sephacryl S200; GE Healthcare) using S200 buffer (10 mM HEPES pH 8.0, 300 mM NaCl, 5 mM dithiothreitol, 5% (w/v) glycerol). Fractions containing monodisperse protein were then pooled and concentrated to ~500 μM, as determined by $A_{280\ nm}$ measurements upon denaturation in 8 M guanidine hydrochloride. Concentration was calculated based on the predicted extinction coefficient (ProtParam, Swiss Institute for Bioinformatics). Additional details regarding protein purification for crystallography can be found online at the SGC Oxford website. Human RGS16 constructs, C-terminal biotinylated $G\alpha_{i1}$, N-terminal deleted (ΔN30) $G\alpha_{i1}$, CFP-$G\alpha_{i1}$, and $G\alpha_{i3}$ were purified exactly as previously described (20, 28, 29).

Single Turnover GTPase Assays—Single turnover [γ-^{32}P]GTP hydrolysis assays were conducted using recombinant $G\alpha_{i1}$ and various concentrations of RGS proteins as previously described (20). Briefly, 100 nM $G\alpha_{i1}$ in reaction buffer (50 mM Tris pH 7.5, 0.05% $C_{12}E_{10}$, 1 mM dithiothreitol, 10 mM EDTA, 100 mM NaCl, and 5 μg/ml bovine serum albumin) was incubated for 10 min at 30 °C with 1×10^6 cpm (2 nM) of [γ-^{32}P]GTP (specific activity of 6500 dpm/Ci). The reaction was then chilled on ice for 5 min prior to the addition of 10 mM $MgCl_2$ and 100 μM unlabeled GTPγS (final concentration) with or without added RGS protein. Reactions were kept on ice and 100-μl aliquots were taken at the indicated time points, quenched in 900 μl of charcoal slurry, and centrifuged before 600-μl aliquots of supernatant were counted via liquid scintillation.

Surface Plasmon Resonance—Optical detection of protein-protein interactions by surface plasmon resonance (SPR) was performed using a Biacore 3000 (GE Healthcare) exactly as previously described (20, 29, 30).

Förster Resonance Energy Transfer (FRET)-based Binding Assays—Förster resonance energy transfer was used to measure binding between $G\alpha_{i1}$ and the triple point mutant RGS2 (C106S,N184D,E191K) as previously described (26, 28). In brief, FRET between recombinant $G\alpha_{i1}$-CFP and YFP-RGS2(C106S,N184D,E191K) proteins was measured using a SpectraMax Gemini fluorescence reader (Molecular Devices, Sunnyvale, CA) using an excitation wavelength of 433 nm (455 nm cutoff) and emission scans from 470 to 535 nm at 2-nm intervals.

Structure Determination—Purified $G\alpha$ and RGS2(C106S, N184D,E191K) proteins were mixed at a molar ratio of 1:1.5 and incubated at 4 °C for 20 min. The sample was passed through an S200 gel filtration column pre-equilibrated with 25 mM HEPES, pH 7.5, 150 mM NaCl, 5% glycerol, 2 mM dithiothreitol, 100 μM $AlCl_3$, 20 mM sodium fluoride, and 100 μM GDP. Protein fractions that eluted as a complex were identified using SDS-PAGE and the fractions were pooled and concentrated to 23 mg/ml prior to crystallization condition screens using a 150-nl drop volume with an TTP Labtech Mosquito nanoliter liquid-handling system. The crystal of the RGS2(C106S,N184D,E191K)-$G\alpha_{i3}$ complex used for data collection was crystallized by vapor diffusion in sitting drops of 400 nl of protein and 200 nl of reservoir solution containing 0.1 M HEPES, pH 7.5, and 2 M ammonium sulfate (TTP Labtech Mosquito).

After cryoprotection in a solution of 2 M ammonium sulfate, 0.1 M HEPES, pH 7.5, and 20% (w/v) D-glucose, crystals were flash cooled in liquid nitrogen. A complete data set was col-

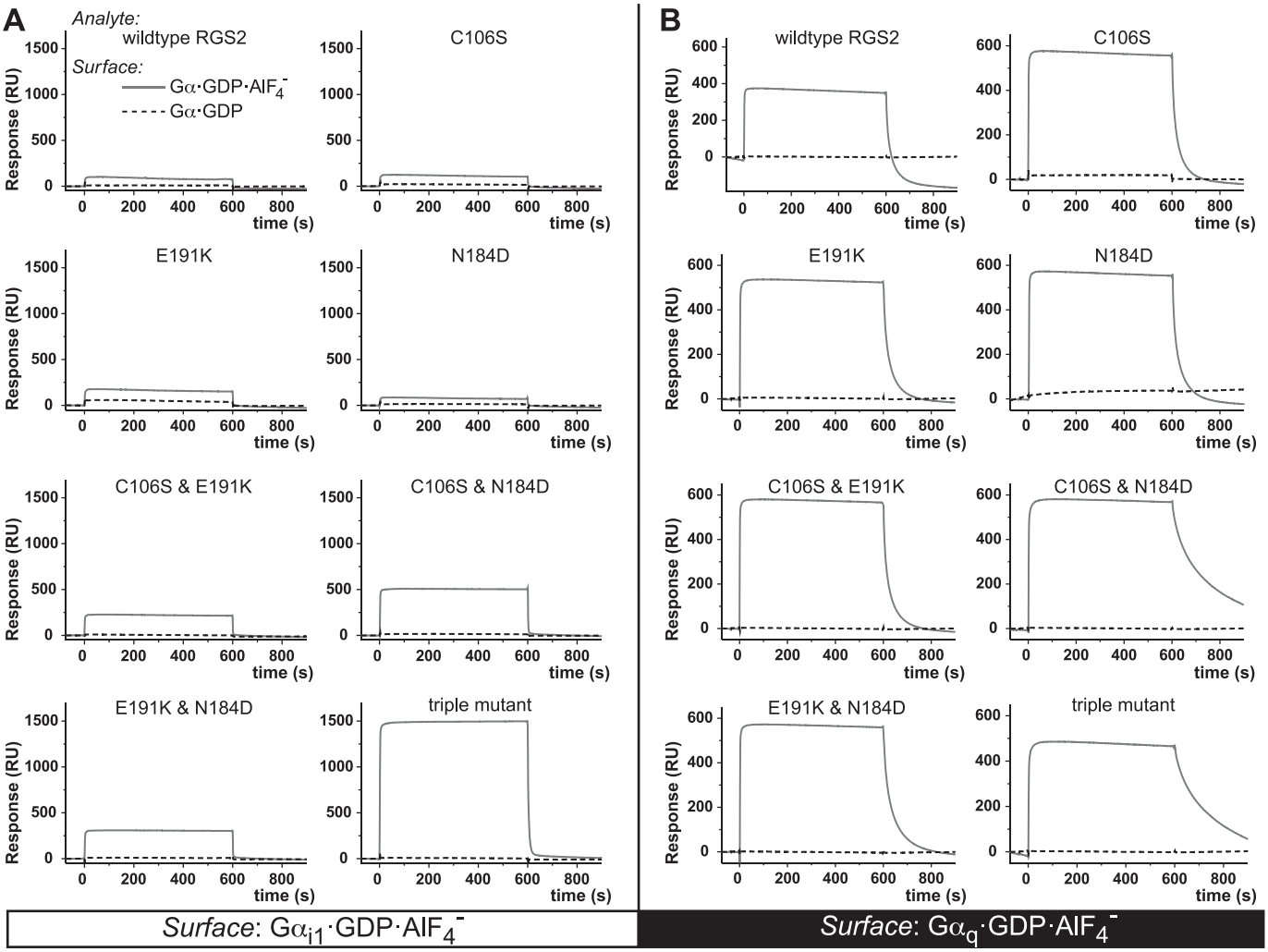

FIGURE 1. **$G\alpha_{i1}$ and $G\alpha_q$ selectivity of wild type RGS2 *versus* RGS2 point mutants profiled by SPR.** $G\alpha_{i1}$-biotin (*left*) or His_6-$G\alpha_q$ (*right*) were immobilized on sensor surfaces for binding analyses of the indicated RGS2 protein analytes (3 μM final concentration). Analyte injections were performed at a flow rate of 20 μl/min for 600 s (start time = 0 s) over surfaces of Gα subunits in the inactive state (GDP-bound; *dashed lines*) or in the transition state for GTP hydrolysis (*i.e.* GDP·AlF_4^--bound; *solid lines*). Legend in *panel A* also applies to sensorgrams of *panel B*.

lected at 100 K on a Rigaku/MSC FR-E rotating anode x-ray generator equipped with an R-AXIS HTC image plate detector. Diffraction images were evaluated with MOSFLM (31), and data were scaled using SCALA (32). The crystal belonged to the space group $P3_221$ with unit cell dimensions $a = 114.54$ Å, $b = 114.54$ Å, and $c = 99.33$ Å. A molecular replacement solution was found in this space group using PHASER (33) with the RGS10/$G\alpha_{i3}$ complex (PDB code 2IHB) as the search model. The RGS2 coordinates from PDB code 2AF0 were superimposed onto the RGS10 coordinates of the RGS10/$G\alpha_{i3}$ positioned complex and rigid body refinement into the electron density was performed using REFMAC5 (34). Difference density in the GDP binding site was modeled using the higher resolution structure of $G\alpha_{i3}$ in the RGS8/$G\alpha_{i3}$ complex (PDB code 2ODE) with one molecule of GDP, a tetrafluoroaluminate ion, and a magnesium ion coordinated by two additional water molecules. Several rounds of manual rebuilding in COOT (35) and restrained refinement with REFMAC5 (34), using Translation/Libration/Screw (TLS) groups calculated with TLSMD (36), resulted in the final structural model described in Table S1. Coordinates of the RGS2(C106S,N184D,E191K)-$G\alpha_{i3}$ complex were deposited in the Protein Data Bank with entry code of 2V4Z.

Cellular cAMP Signaling Assays—HEK293T cells were transfected using Lipofectamine 2000 (Invitrogen) in 6-well dishes with 4 μg of total DNA including pGloSensor™-20F cAMP biosensor plasmid (Promega Corp., Madison WI), dopamine D2 receptor, and empty vector, HA-RGS2(WT), or HA-RGS2(C106S,N184D,E191K). The RGS2 expression vectors encoded solely the RGS domain (amino acid Lys^{71}–His^{209}; with an N-terminal HA epitope tag) to avoid the influence of non-RGS domain regions on adenylyl cyclase function (*e.g.* Ref. 37). Twenty-four hours post-transfection, cells were re-plated on poly-D-lysine-treated, clear-bottom, white 96-well plates at a density of 60,000 cells/well. Forty-eight hours post-transfection, culture medium was aspirated and cells were washed once with assay medium (Dulbecco's modified Eagle's medium with 10% fetal bovine serum (without phenol), 15 mM HEPES, pH 7.4) before being incubated for 2 h with 40 μl/well of equilibration medium (assay medium with 4% GloSensor™ substrate). After 2 h, 6.6 μl of 6× final concentration of quinpirole (diluted in 10 μM forskolin-containing assay medium) was added to

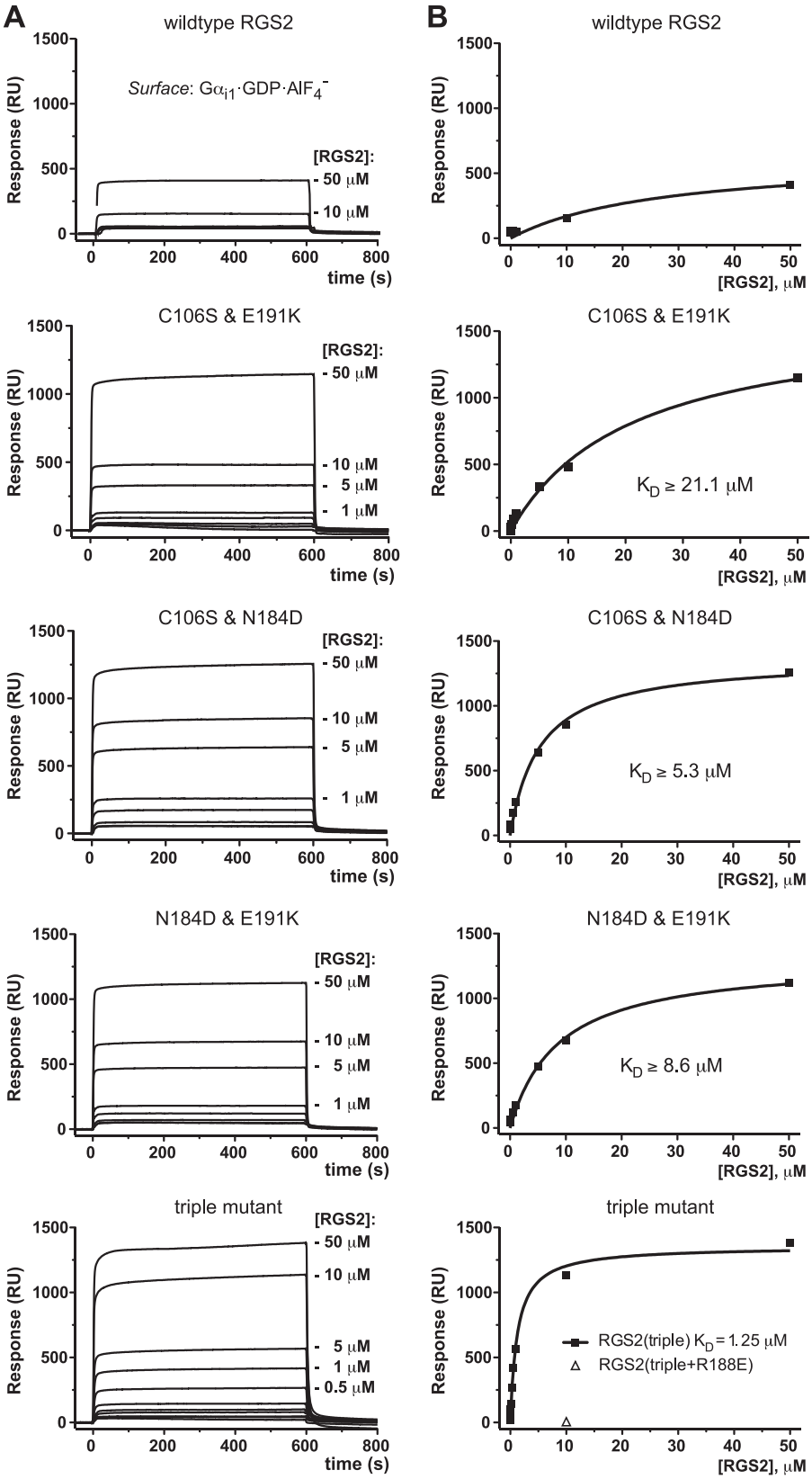

FIGURE 2. **Quantitation of RGS2 binding to $G\alpha_{i1}$.** SPR was performed as described in the legend to Fig. 1, with the concentration of the RGS2 analyte titrated from 1 nM to 50 μM. Sensorgrams were subsequently used in equilibrium saturation binding analyses to determine RGS2/$G\alpha_{i1}$ interaction binding affinities. Dissociation constants (K_D values) were estimated to be ≥21.1 (95% CI, 11.6–30.7 μM), ≥5.3 (95% CI 3.1–7.5 μM), and ≥8.6 (95% CI 5.4–11.9 μM) for the double mutants RGS2(C106S,E191K), RGS2(C106S,N184D), RGS2(N184D,E191K), respectively, and determined to be 1.25 (95% CI, 1.0–1.6 μM) for the triple mutant RGS2(C106S,N184D,E191K). A K_D value for the wild type RGS2/$G\alpha_{i1}$ interaction could not be estimated because saturation was not obtained at concentrations tested.

each well and allowed to incubate for 10 min before GloSensor emission was read on a MicroBeta Plate Counter (PerkinElmer). Before plotting, luminescence counts were normalized to 100% maximal response for each condition to account for variability in GloSensor expression, transfection efficiency, and the exact number of cells per well.

RESULTS AND DISCUSSION

Evaluating Point Mutations to RGS2 That Facilitate Interaction with $G\alpha_{i1}$—RGS2 is the only member of the R4-subfamily known to bind specifically to $G\alpha_q$ and not to $G\alpha_{i/o}$ heterotrimeric G-protein subunits *in vitro* (20, 21). Three amino acids within RGS2 were identified by Heximer and colleagues (21) as potential selectivity determinants in studies of $G\alpha_o$-directed GAP activity by RGS domain chimera derived from RGS2 and RGS4 sequences: namely, cysteine 106, asparagine 184, and glutamate 191. In the present study, we mutated these three amino acids to the highly conserved corresponding amino acids in R4-subfamily members (Cys^{106} to serine, Asn^{184} to aspartate, and Glu^{191} to lysine; supplementary Fig. S1) to identify their respective contributions to Gα substrate specificity.

RGS2 proteins containing these point mutations, either singly, in tandem, or all three together, were expressed in *E. coli* and purified to homogeneity (Fig. S2). SPR spectroscopy was used (*e.g.* Fig. 1) to assess if any individual mutation, or combination of point mutations, was capable of changing the selectivity of RGS2. All mutants retained wild type binding toward $G\alpha_q$ (*e.g.* Fig. 1*B*). Single mutations to RGS2 (C106S, N184D, or E191K) did not enhance binding to $G\alpha_{i1}$ and only minimal enhancements to binding were observed with the C106S, N184D, C106S,N191D, and E191K, N184D double mutants (*e.g.* Fig. 1*A*); in contrast, the triple mutant RGS2 exhibited a dramatic increase in $G\alpha_{i1}$ binding *versus* wild type

RGS2. Although the magnitude of binding of the RGS2 double mutants was significantly less than that observed with the triple mutant, binding isotherms were nonetheless generated for all double mutants along with the triple mutant by injecting increasing concentrations of RGS2 protein over the $G\alpha_{i1}$·GDP·AlF_4^- surface. Using equilibrium binding analyses (Fig. 2), dissociation constants (K_D values) for the RGS2/$G\alpha_{i1}$·GDP·AlF_4^- interaction were estimated to be ≥5.3, ≥8.6, and ≥21.1 μM, for C106S,N184D, E191K,N184D, and C106S,E191K, respectively, whereas the K_D value was determined to be 1.25 μM for the RGS2(C106S,N184D,E191K) triple mutant. Dissociation constants derived for the RGS2 double mutants are likely underestimated given an inability to attain saturating concentrations of these particular RGS2 analytes and thereby attain maximal binding (B_{max}).

To determine whether the enhanced affinity of the RGS2 triple mutant was the result of improvements to a canonical RGS domain/Gα interaction interface, a highly conserved, surface-exposed arginine within this canonical interface (Arg^{188} in the αVIII helix; Fig. S1) was mutated to glutamic acid. As has been shown for other RGS proteins (38), this single charge-reversal point mutation (R188E) on the Gα-binding surface of the RGS2 triple mutant abolished binding to $G\alpha_{i1}$·GDP·AlF_4^- (Fig. 2*B*, *bottom panel*).

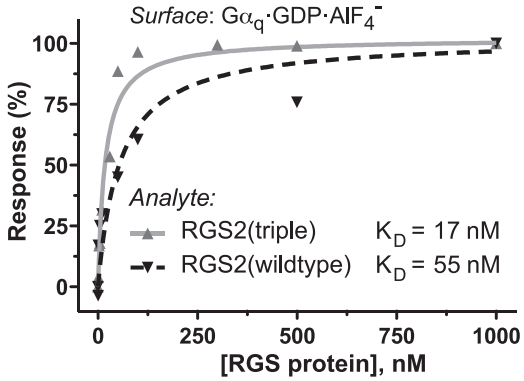

FIGURE 3. **Quantification of RGS2 binding to $G\alpha_q$.** SPR was performed as described in the legend to Fig. 1, using an immobilized His_6-$G\alpha_q$·GDP·AlF_4 surface and RGS2 analyte concentrations from 0.5 to 1000 nM. Using equilibrium saturation binding analyses, RGS2/$G\alpha_q$ dissociation constants were determined to be 55 nM (95% CI, 23.4–86.9 nM) for wild type RGS2 and 17 nM (95% CI, 8.7–27.0 nM) for the RGS2(C106S,N184D,E191K) triple mutant.

To quantify any difference in the ability of the RGS2(C106S,N184D,E191K) triple mutant to bind $G\alpha_q$, increasing concentrations of wild type RGS2 and RGS2 triple mutant proteins were separately injected over an immobilized $G\alpha_q$·GDP·AlF_4^- surface (Fig. 3). Dissociation constants were determined to be 55 nM (95% confidence interval (CI) of 23–87 nM) and 17 nM (95% CI, 9–27 nM) for wild type RGS2- and RGS2(C106S,N184D,E191K)-bound $G\alpha_q$, respectively.

To confirm these SPR-derived results with an orthogonal technique of assessing the RGS domain/Gα interaction, FRET measurements were performed using a YFP-RGS2 (C106S, N184D,E191K)/$G\alpha_{i1}$-CFP pair, similar to the RGS4/$G\alpha_{i1}$ interaction FRET assay we have previously described (28). In the presence of GDP, aluminum tetrafluoride, and Mg^{2+} ("AMF"), binding between RGS protein and the Gα subunit is observed as an increase in YFP emission and decrease in CFP emission; in the presence of GDP alone, no binding is observed as expected (28, 39) and so the ratio of YFP to CFP emission remains low. The relative affinities of wild type RGS2, RGS16, and RGS2 triple mutant were assessed by using this FRET binding assay in a competitive manner: unlabeled RGS protein was added in increasing amounts to a fixed concentration of YFP-RGS2(C106S,N184D,E191K) and $G\alpha_{i1}$-CFP proteins. As expected, only unlabeled RGS2(C106S,N184D, E191K) and RGS16 proteins were able to inhibit the binding of the RGS2(C106S,N184D,E191K)/$G\alpha_{i1}$ FRET pair (Fig. 4), with observed IC_{50} values of 526 nM (95% CI, 236–1171 nM) and 115 nM (78–168 nM), respectively. At no concentration tested was wild type RGS2 able to inhibit binding of the RGS2(C106S,N184D,E191K)/$G\alpha_{i1}$ FRET pair (Fig. 4*B*), consistent with the lack of affinity between wild type RGS2 and $G\alpha_i$ subunits seen in our present SPR analyses and previously published studies (20, 21).

Determinants of RGS2 GAP Activity on $G\alpha_{i1}$ in Vitro—Using SPR and FRET, we demonstrated that all three point mutations were required to facilitate high affinity binding of RGS2 to $G\alpha_{i1}$. To determine whether this enhanced binding affected the ability of RGS2 to accelerate GTP hydrolysis by $G\alpha_{i1}$, we performed single turnover GTPase assays with both wild type and triple mutant RGS2 proteins (Fig. 5). At no concentration tested was wild type RGS2 capable of increasing GTP hydrolysis over the intrinsic GTP hydrolysis rate of $G\alpha_{i1}$ (Fig. 5*A*). In contrast, a substoichiometric amount of RGS16 (a known $G\alpha_{i1}$ GAP; Ref. 40) was able to accelerate $G\alpha_{i1}$ GTPase activity; complete hydrolysis of bound GTP was observed in less than 15 s at 0 °C. Unlike wild type RGS2, the RGS2(C106S,N184D,E191K) triple mutant was able to increase the rate of $G\alpha_{i1}$ GTP hydrolysis in a dose-dependent manner (Fig. 5*B*); however, adding the R188E mutation to

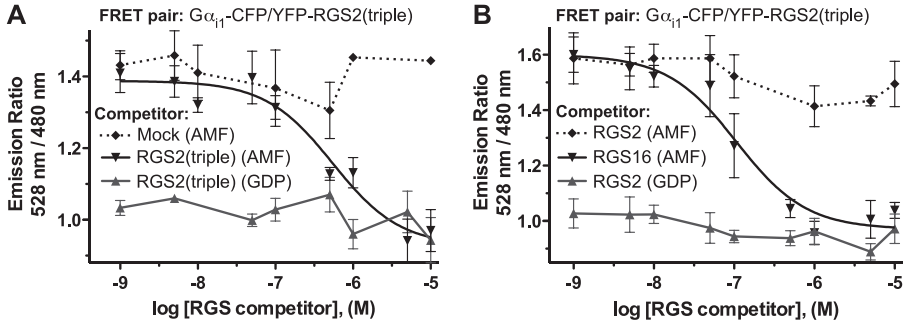

FIGURE 4. **Competition FRET assays of the $G\alpha_{i1}$-CFP/YFP-RGS2(triple) interaction.** *A*, the fusion proteins YFP-RGS2(C106S,N184D,E191K) and $G\alpha_{i1}$-CFP interact in the presence of GDP and AlF_4·Mg^{2+} ("AMF") but not in the presence of GDP alone. This interaction can be inhibited by the addition of unlabeled RGS2(C106S,N184D,E191K) "triple" mutant protein (IC_{50} value of 526 nM; 95% CI, 236–1171 nM), but not by the addition of buffer alone. *B*, the addition of unlabeled wild type RGS2 to the $G\alpha_{i1}$-CFP/YFP-RGS2(triple mutant) FRET pair does not result in a decrease in FRET; however, the addition of RGS16 (known to have affinity for $G\alpha_{i1}$ (20) competitively inhibits binding (IC_{50} value of 115 nM; 95% CI, 78–168 nM).

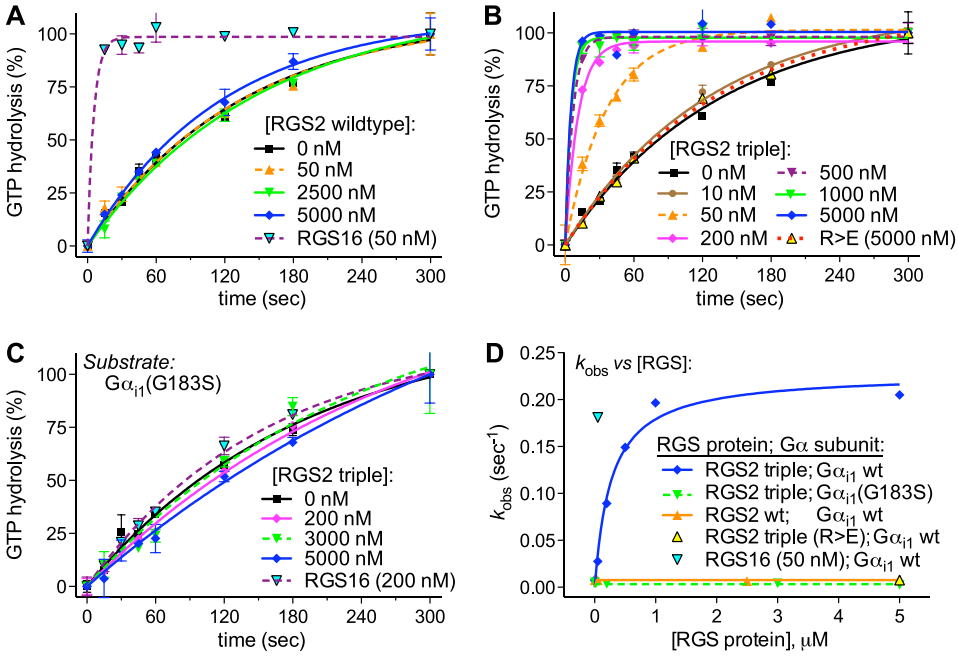

FIGURE 5. **The triple mutant RGS2(C106S,N184D,E191K), but not wild type RGS2, accelerates the GTP hydrolysis rate of $G\alpha_{i1}$.** *A*, increasing concentrations of wild type RGS2 (as indicated) are unable to accelerate the GTP hydrolysis of 200 nM $G\alpha_{i1}$. Intrinsic GTP hydrolysis by isolated $G\alpha_{i1}$ (k_{obs}) was measured at 0.0075 s^{-1} (95% CI 0.0055–0.010 s^{-1}), whereas k_{obs} values of 0.0076 (0.0055–0.0097), 0.0066 (0.0054–0.0078), and 0.0086 (0.0069–0.010) s^{-1} were observed upon the addition of 50, 2500, or 5000 nM wild type RGS2, respectively. RGS16 is a potent GAP for $G\alpha_i$ subunits (*e.g.* Ref. 20) and, at substoichiometic concentrations (50 nM), was found to accelerate GTP hydrolysis by $G\alpha_{i1}$: k_{obs} of at least 0.18 s^{-1} (an underestimate as the measurement is limited by sampling time constraints). *B*, the triple mutant RGS2(C106S,N184D,E191K) was observed to accelerate GTP hydrolysis by 200 nM $G\alpha_{i1}$ in a dose-dependent manner: k_{obs} values of 0.0075 (0.0055–0.0095), 0.0079 (0.0068–0.0089), and 0.028 (0.023–0.032) s^{-1} were observed upon the addition of 0, 10, and 50 nM RGS2(triple) protein, respectively. Higher concentrations of RGS2(triple) protein (200, 500, 1000, and 5000 nM) led to GTPase rates of at least 0.1–0.2 s^{-1} (again underestimated due to sampling time constraints). The triple mutant also containing a fourth, loss-of-function point mutation (namely, RGS2(C106S,N184D,E191K,R188E)) was unable to accelerate GTP hydrolysis by $G\alpha_{i1}$: with a k_{obs} value of 0.0076 (0.0066–0.0086) s^{-1}. *C*, the single point mutation to $G\alpha_{i1}$ (glycine 183 to serine, G183S (41)) renders $G\alpha_{i1}$ insensitive to the GAP activity of RGS proteins. The intrinsic hydrolysis rate of the $G\alpha_{i1}$(G183S) mutant was determined to be 0.0053 (0.0037–0.0069) s^{-1}. Upon addition of 200, 3000, or 5000 nM of the RGS2(C106S,N184D,E191K) triple mutant, the k_{obs} was found to be 0.0036 (0.0026–0.0046), 0.0042 (0.0060–0.0078), and 0.0025 (0.00017–0.0048) s^{-1}, respectively; the k_{obs} for GTP hydrolysis after addition of 200 nM RGS16 was observed to be 0.0064 (0.0052–0.0076) s^{-1}. *D*, the k_{obs} values are plotted *versus* concentration of RGS protein to demonstrate the dose-dependent increase in GAP activity upon the addition of RGS2(C106S,N184D,E191K) protein to wild type $G\alpha_{i1}$, but not the RGS-insensitive $G\alpha_{i1}$(G183S) mutant.

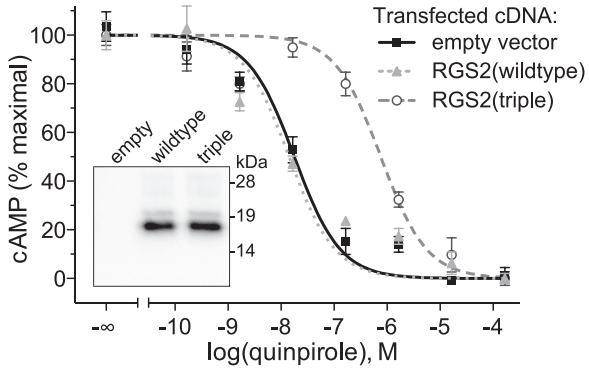

FIGURE 6. **The triple mutant RGS2(C106S,N184D,E191K), but not wild type RGS2, inhibits dopamine D2-receptor influence on forskolin-stimulated cAMP production.** HEK293T cells were transiently co-transfected with expression vectors for the GloSensor cAMP biosensor and the G_i-coupled dopamine D2-receptor with empty vector, wild type RGS2, or the RGS2(triple) mutant. Inhibition of forskolin-stimulated cAMP production was determined after activation of the D2 receptor with various concentrations of quinpirole as indicated. The IC_{50} (95% CI) for quinpirole was determined to be 18 (12–26), 14 (9–22), and 762 (498–1170) nM in the presence of empty vector, wild type RGS2, and the triple mutant, respectively. *Inset*, post-transfection cell lysates were immunoblotted with anti-HA epitope tag antibody to confirm the equivalent overexpression of HA-RGS2 and HA-RGS2(C106S,N184D,E191K) proteins.

the triple mutant resulted in a complete loss in GAP activity, consistent with the loss of $G\alpha_{i1}$ binding observed in SPR and FRET assays. To further confirm that the mechanism of action of the RGS2(C106S, N184D,E191K) triple mutant in increasing GTP hydrolysis by $G\alpha_{i1}$ was related to a canonical RGS domain/$G\alpha$ interaction and not the inadvertant addition of a contaminating GTPase, we assessed the effects of both RGS2(C106S, N184D,E191K) and RGS16 proteins on an RGS-insensitive $G\alpha_{i1}$ point mutant: specifically, G183S in the $G\alpha$ switch I region (41). Neither RGS2(C106S,N184D,E191K) nor RGS16 proteins were able to increase the intrinsic rate of GTP hydrolysis exhibited by this RGS-insensitive $G\alpha_{i1}$ (Fig. 5, *C* and *D*).

Determinants of RGS2 Activity on G_i-coupled GPCR Signaling in Cells—To validate in a cellular context the change in $G\alpha$ specificity exhibited *in vitro* by the RGS2(C106S, N184D,E191K) triple mutant, we used an intracellular cAMP biosensor to measure G_i heterotrimer-mediated inhibition of forskolin-stimulated cAMP production in HEK293T expressing the G_i-coupled D2 dopamine receptor along with either wild type RGS2 or the RGS2(C106S,N184D,E191K) mutant. Upon treatment of transfected cells with forskolin, a robust increase in luminescence was observed from the cAMP sensor, reflecting direct activation of adenylyl cyclase by forskolin (4); upon administration of the dopamine D2/D3-receptor selective agonist, quinpirole, dose-dependent inhibition of this cAMP production was observed. Wild type RGS2 had no effect on the IC_{50} of quinpirole (Fig. 6). However, cellular expression of the RGS2(C106S,N184D,E191K) triple mutant resulted in a significantly higher IC_{50} for quinpirole (762 *versus* 18 nM for empty vector; Fig. 6), indicating that the gain of $G\alpha_i$-directed activity is readily apparent in a cellular context as well as *in vitro* for the RGS2 triple mutant.

Structural Determinants of RGS2 Interaction with $G\alpha$ Subunits—To determine the structural basis for the $G\alpha$ selectivity of RGS2, we used x-ray crystallography to obtain a structural model of the RGS2 triple mutant bound to a $G\alpha_i$ subunit. A diffraction pattern data set was collected on a single crystal containing a complex between the RGS2(C106S,N184D, E191K) triple mutant and $G\alpha_{i3}$·GDP·AlF_4^- and was refined to 2.8-Å resolution (supplemental Table S1). The resultant structural model revealed canonical RGS domain/$G\alpha$ interactions

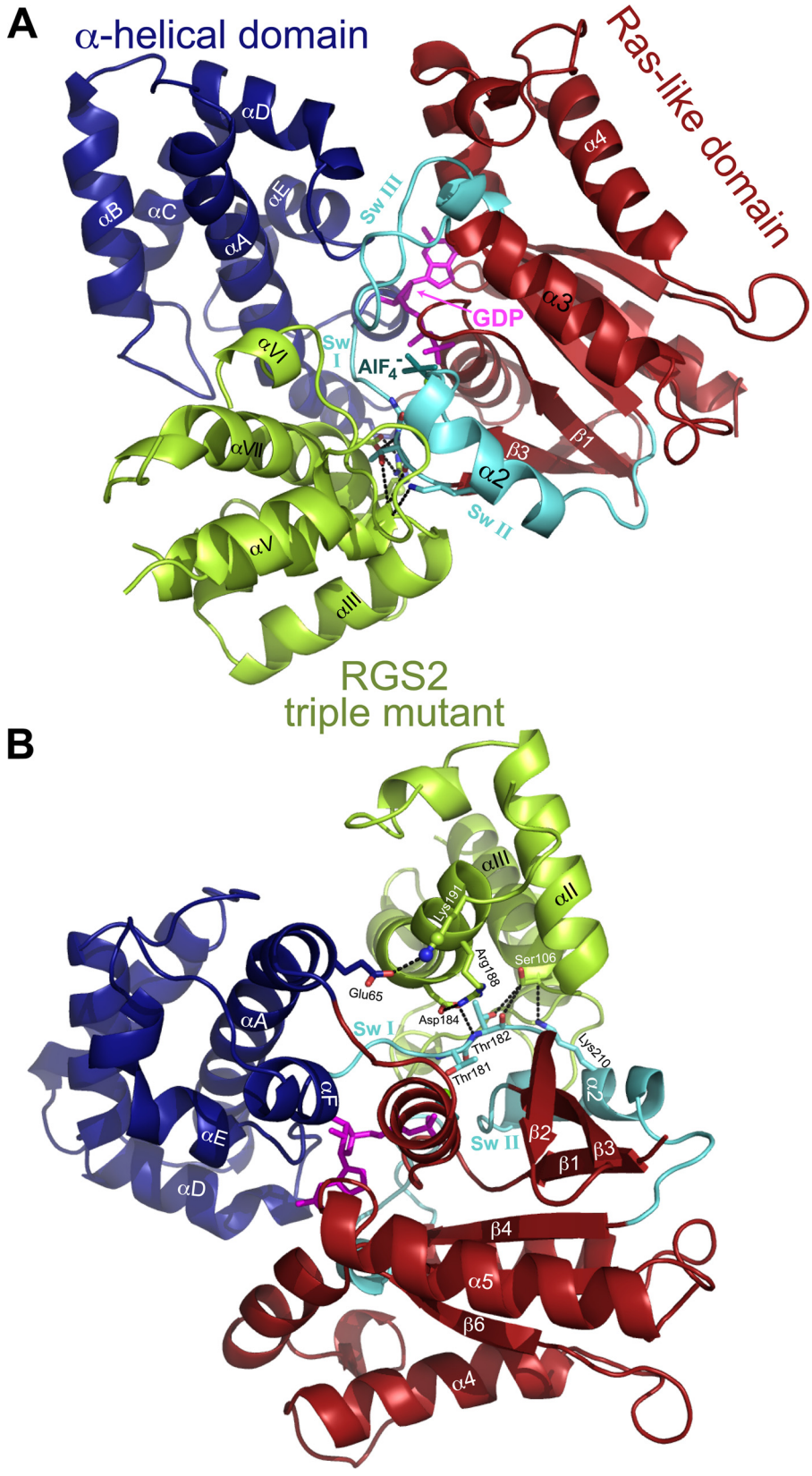

FIGURE 7. **Overall structural features of the RGS2(C106S,N184D,E191K)-$G\alpha_{i3}$·GDP·AlF_4^- complex.** *A*, the tertiary structure of $G\alpha_{i3}$ is composed of a Ras-like domain (*red*) and an all α-helical domain (*blue*) and is present in a transition-state mimetic form bound to a molecule of GDP (*magenta*) and tetrafluoroaluminate (AlF_4^-) ion (*gray/blue sticks*). The three critical switch regions of Gα (numbered *Sw I* to *Sw III*) are colored *cyan*. All three switch regions are engaged by the RGS2 RGS domain (*yellow-green*). *Panel B* represents the same structural model as in *panel A*, but rotated to highlight contacts made by residues serine 106, aspartate 184, and lysine 191 of the RGS2(C106S,N184D,E191K) triple mutant. This same orientation of the complex is presented in Fig. 8*B*.

(20, 42), specifically, contacts between the flexible switch regions of $G\alpha_{i3}$ and the nine α-helical bundle formed by the RGS2 triple mutant (Fig. 7).

One of the three mutation sites within the RGS2 triple mutant, aspartate 184, is observed to form a double salt bridge (Fig. 8*A* and Fig. S3) with the neighboring arginine 188, the latter being an αVIII residue completely conserved among all other R4-subfamily RGS domains (Fig. S1). Asparagine 184 of wild type RGS2, located between helix αVII and αVIII, is an aspartic acid in all other R4-subfamily RGS domains (Fig. S1). The additional terminal oxygen present in the aspartate side chain (and missing in asparagine) normally allows two salt bridges to be formed (Fig. 8*A*) with the conserved αVIII helix arginine residue (*e.g.* Arg^{170} of RGS16, Arg^{188} of RGS2). These salt bridges are not consistently observed in all unliganded RGS domain structures (20); however, this double salt bridge is present in all R4-subfamily RGS domains complexed with $G\alpha_{i/o}$ subunits (Table S2), suggesting that their formation is important for making the RGS domain competent to bind $G\alpha_{i/o}$ subunits. The importance of this Arg-Asn side chain interaction is supported by the loss of $G\alpha_i$ binding and $G\alpha_i$-directed GAP activity when this αVIII helix arginine is mutated to glutamate (Figs. 2 and 5). The significance of this intramolecular interaction is further supported by observations that mutating the analogous αVIII helix arginine in RGS4 (Arg^{167}) and RGS12 (Arg^{821}) results in loss of $G\alpha_{i/o}$ binding and $G\alpha_{i/o}$-directed GAP activity (38, 43, 44). Although Arg^{188} of RGS2 does not make any critical contacts with $G\alpha_{i3}$ *per se*, it has a critical role in orienting Asp^{184} (Fig. 8*B*) to form a conserved hydrogen bond with the main chain amide of a threonine residue in the Gα switch I region (Thr^{182} of $G\alpha_i$ (20, 42); Thr^{183} of $G\alpha_o$ (45)). In the structure of wild type, uncomplexed RGS2 (PDB code 2AF0; Ref. 20), asparagine at this position (Asn^{184})

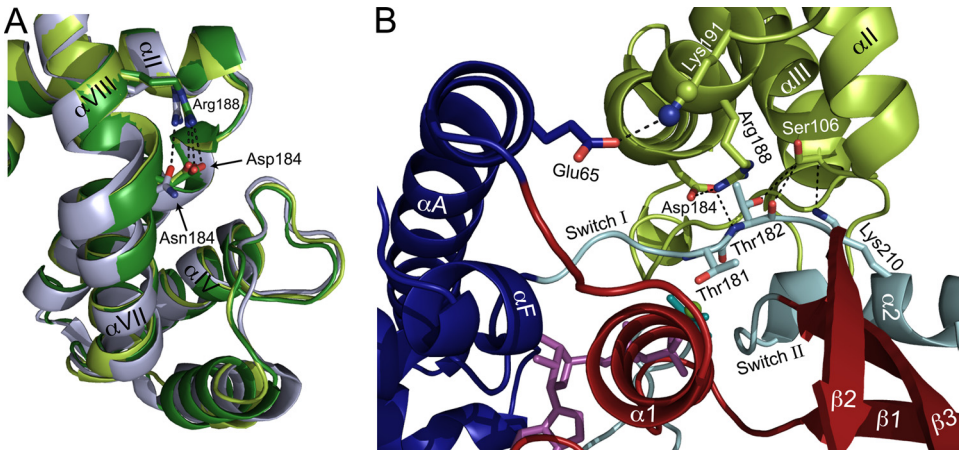

FIGURE 8. **Particular Gα selectivity determinants inferred from the structural model of the triple mutant RGS2(C106S,N184D,E191K) bound to $G\alpha_{i3}$.** *A*, illustration of the αVII–αVIII region of the RGS domain to highlight the intramolecular interaction between the highly conserved αVIII helix arginine (Arg^{188} of RGS2) and position 184 (asparagine in wild type RGS2 and aspartate in the triple mutant). RGS2(C106S,N184D,E191K) triple mutant (*yellow-green*; PDB code 2V4Z), unliganded wild type RGS2 (*gray*; PDB code 2AF0), and the $G\alpha_{i1}$-bound RGS16 (*dark green*; PDB code 2IK8) were aligned by sequence and then structure (Cα atoms) using the Align command with default align settings of MacPyMOL (DeLano Scientific, Palo Alto, CA), resulting in root mean square deviations of 0.92 and 0.80 Å, respectively. The conserved Arg^{188} makes salt bridges with the terminal oxygens of the Asp^{184} side chain in the RGS2(C106S,N184D,E191K) mutant and the analogous aspartate side chain in RGS16; however, only one contact can be made between Arg^{188} and the Asn^{184} side chain of wild type RGS2. Loss of the second salt bridge creates a torsion in the wild type RGS2 Asp^{184} residue, resulting of the loss of the stabilizing hydrogen bond to Thr^{182} in switch I of the Gα subunit. *B*, critical contacts between the three mutated positions of RGS2(C106S,N184D,E191K) (*yellow-green*) and its Gα binding partner (Ras-like domain in *red*; all-helical domain in *blue*; switch regions in *cyan*; bound GDP in *magenta*). The modeled terminal atoms of the Lys^{191} side chain (*spheres*) within RGS2(C106S,N184D,E191K) are in close enough proximity to make a hydrogen bond with Glu^{65} of the Gα all-helical domain. Asp^{184} makes two hydrogen bonds with Arg^{188} and an additional bond with the backbone amine of the peptide bond connecting Thr^{181} and Thr^{182}, both located within switch I of Gα. Ser^{106} of the RGS2 triple mutant is tightly packed with the backbone carbonyl and γ-hydroxyl of Gα Thr^{182}, both being less than 3.9 Å from β-carbon of Ser^{106}. Additionally, the Gα switch II residue Lys^{210} is 3.8 Å from the Ser^{106} α-carbon.

forms only a single hydrogen bond with terminal amine of Arg^{188} and, rotated in this manner, the side chain cannot at the same time form a hydrogen bond with the Thr^{182} backbone (Fig. 8*A* and Table S2).

The aspartate substitution at position Asn^{184} is critical to allow binding of RGS2 to $G\alpha_i$; however, this single substitution alone is not sufficient to engender robust $G\alpha_i$ binding (Fig. 1). Ser^{106} is completely conserved among all R4-subfamily RGS domains except RGS2, in which this position is a cysteine residue (Fig. S1). Mutating Cys^{106} to serine was also necessary to obtain high affinity binding to $G\alpha_i$ subunits (Figs. 1 and 2); whereas the Ser^{106} side chain was not observed in the structural model to make any critical contacts with $G\alpha_{i3}$, this residue is tightly packed among other residues (Fig. 8*B*). The structure of the RGS2(C106S,N184D,E191K)-$G\alpha_{i3}$ complex reveals that the β-carbon of Ser^{106} is closely juxtaposed with the backbone carbonyl and γ-hydroxyl of Thr^{182} within switch I of $G\alpha_{i3}$; additionally, the α-carbon of Ser^{106} is 3.8 Å from the terminal amine of Lys^{210} within switch II of $G\alpha_{i3}$. In conjunction with the SPR binding data, the observed tight packing of Ser^{106} within the RGS2(C106S,N184D,E191K)-$G\alpha_{i3}$ complex suggests that the Cys^{106} residue of wild type RGS2 prevents high affinity binding to $G\alpha_i$ subunits by steric blockade of interactions with switch I and switch II of the Gα subunit.

Although amino acid positions 106 and 184 are completely conserved among all R4-subfamily RGS domains except RGS2, the specific amino acid at position 191 is conserved only in its basic character, being either a lysine or an arginine in all R4-subfamily RGS domains (Fig. S1). In wild type RGS2, this position is instead an acidic residue (glutamate 191). In the structural data derived from the RGS2(C106S, N184D,E191K)-$G\alpha_{i3}$ complex, electron density was present only for the α-, β-, and γ-carbons of the mutated Lys^{191}; however, the final ordered carbon atom was found to be only 5.1 Å from the hydroxyl oxygen of Glu^{65} in the αA helix of the $G\alpha_{i3}$ all-helical domain. Electron density was present to fit the Cα, Cβ, Cγ, and Cδ atoms of the Lys^{191} residue (Fig. S3). The Cε and terminal amine were modeled by superimposing a Lys over those parts of the carbon atom chain that could be placed with electron density, revealing that this basic side chain would be less than 3.0 Å from the hydroxyl oxygen of $G\alpha_{i3}$ Glu^{65} and thus within hydrogen bonding distance. It is possible that the high salt concentration necessary for crystallization screened the electrostatic contribution of this interaction away, resulting in a partially disordered side chain. In wild type RGS2, this salt bridge would be lacking and this position instead would create electrostatic repulsion between RGS2 Glu^{191} and the all-helical domain of $G\alpha_{i3}$. The importance of all-helical domain contacts to RGS protein selectivity for Gα substrates has been previously speculated for the retinal-specific proteins RGS9-1 and Gα-transducin (46); our present finding with RGS2 provides one of the first structural insights into these interactions. These RGS domain/all-helical domain interactions, whereas typically underappreciated when considering the structural determinants of the RGS protein/Gα interaction interface (*e.g.* Refs. 42 and *cf.* 20), may provide a unique point of interdiction to exploit with selective RGS protein inhibitors.

Unique Determinants of RGS2 $G\alpha_q$ Selectivity Are Conserved among Species with Cardiovascular Systems—Current knowledge of Gα selectivity suggests that R4-subfamily members, as well as proteins from the more ancestral RZ-subfamily (*e.g.* RGS17, -19, and -20), can act as GAPs for both $G\alpha_i$ and $G\alpha_q$ subunits (20, 47), with the R4-protein RGS2 particularly attuned to $G\alpha_q$ over $G\alpha_i$. Given its unique Gα selectivity and its specialized role in cardiovascular signal transduction, RGS2 is likely to have arisen from the R4-subfamily in response to the development of cardiovascular structures and function.

In evolutionary terms, $G\alpha_q$ emerged as the harbinger of a distinct and recognizable Gα subfamily in fungi, and $G\alpha_q$ subunits are present in all metazoans including sponges (48, 49). Although RZ-subfamily RGS proteins are represented within the genomes of nematodes and arthropods (50), a distinct R4-subfamily does not appear until the evolution of urochor-

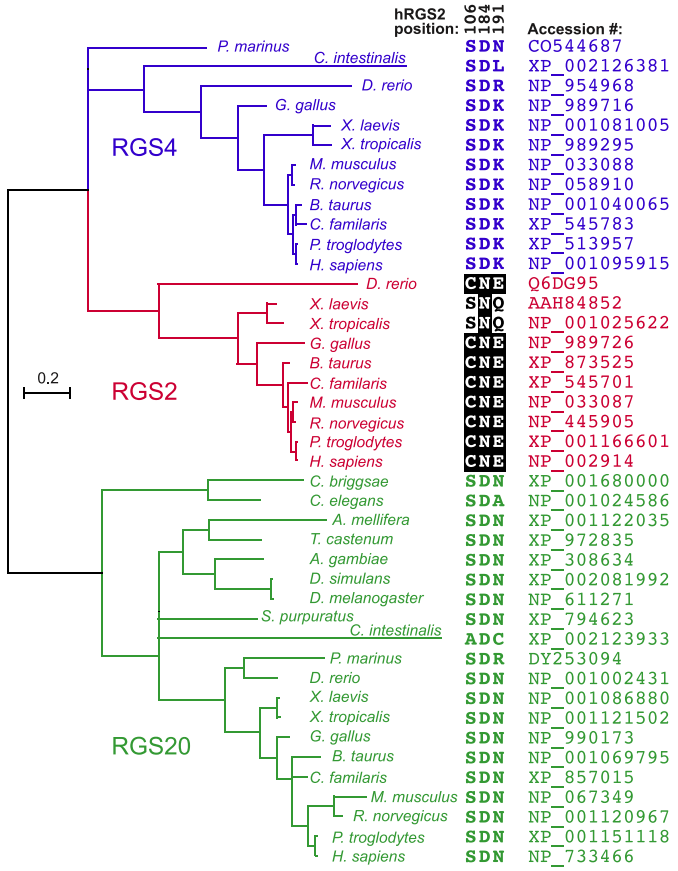

FIGURE 9. **Emergence of the specialized R4-subfamily member RGS2 and evolutionary conservation of its three $G\alpha_q$-selectivity residues.** Full-length, protein open reading frame sequences for RGS2, RGS4, and RGS20 orthologs were obtained from the genomes of the indicated multicellular organisms and aligned using T-Coffee version 1.37 (61). Sequence alignments were manually adjusted using SEAVIEW version 3.2 (62) prior to the generation of a Markov-chain Monte Carlo-based phylogeny using MrBayes version 3.1.2 (Refs. 63 and 64); the dendrogram was visualized using Njplot version 2.3 (65).

dates. The genome of the urochordate *Ciona intestinalis* (sea squirt) encodes at least two RGS proteins (Fig. 7), an ortholog of the ancestral RZ-subfamily progenitor found in nematodes and arthropods, as well as a newly divergent R4-subfamily member (but not an RGS2 ortholog *per se*). With specialized tissues such as a notochord, digestive tract, single chamber heart, and gonads, *C. intestinalis* is commonly considered an excellent modern representative of the precursor to higher vertebrates (51, 52). Agnatha (jawless fish) such as the sea lamprey *Petromyzon marinus* are considered the most primitive extant members of early vertebrates (53) and represent the first vertebrate to exhibit cardiac innervation (54). Although the *P. marinus* cardiovascular system is more advanced than the open system of *C. intestinalis*, it is still considered primitive in that it lacks an elastin-reinforced vasculature (55), coronary circulation, and a pericardial-contained fourth chamber (conus or bulbus arteriosus) to dampen systolic oscillations in blood pressure (54). Similar to *C. intestinalis,* the genome of *P. marinus* encodes at least two RGS proteins, the ancestral RZ member and a single R4 member (Fig. 9); however, no RGS2-like protein has yet been identified in this species.

As chordates evolved into the Gnathostomata (jawed vertebrates), the cardiovascular system rapidly developed coronary vessels, inhibitory vagal innervation, excitatory adrenergic innervation, and responses to prostaglandins, nitric oxide, and endothelin (56). This advance is marked in *Danio rerio* by the addition of multiple R4 proteins, specifically including a $G\alpha_q$-specific RGS2 protein (Fig. 9). This unique member of the R4-subfamily, with cysteine, asparagine, and aspartate at the three key specificity positions, is highly conserved in the extant representatives of all subsequent evolutionary steps: amphibians (*e.g. Xenopus laevis* and *Xenopus tropicalis*), avians (*e.g. Gallus gallus*) and mammals (Fig. 9); the three defining residues are seen to be unique among all R4-subfamily members within a given species (*e.g.* human R4 paralogs aligned in Fig. S1). Only amphibians (*X. laevis* and *X. tropicalis*) do not contain all three RGS2-defining amino acids (Fig. 9): whereas the RGS2 signature residue asparagine is present at position 184, serine (not cysteine) is present at position 106, and a neutral glutamine (not glutamate) is present at position 191. (Note that the latter glutamine is not seen in RGS2, RGS4, nor RGS20 paralogs.) Even though the conservation is not absolute in the amphibians, we have shown that asparagine in position 184 is sufficient on its own to significantly reduce $G\alpha_i$ affinity (*i.e.* ~20-fold; compare K_D of >21 μM for the C106S,E191K RGS2 double mutant *versus* K_D of 1.25 μM for the C106S,N184D,E191K triple mutant in Fig. 2). In conclusion, the conservation of these three key residue positions suggests that RGS2 has indeed evolved from the R4-subfamily to be a specialized $G\alpha_q$ GAP for the modern cardiovascular system by acquiring particular residues at one or more of three key positions that have been highlighted in our mutagenesis/crystallography studies.

Acknowledgments—The Structural Genomics Consortium is a registered charity (number 1097737) that receives funds from the Canadian Institutes for Health Research, the Canadian Foundation for Innovation, Genome Canada through the Ontario Genomics Institute, GlaxoSmithKline, Karolinska Institutet, the Knut and Alice Wallenberg Foundation, the Ontario Innovation Trust, the Ontario Ministry for Research and Innovation, Merck & Co., Inc., the Novartis Research Foundation, the Swedish Agency for Innovation Systems, and the Swedish Foundation for Strategic Research and the Wellcome Trust.

REFERENCES

1. Pierce, K. L., Premont, R. T., and Lefkowitz, R. J. (2002) *Nat. Rev. Mol. Cell Biol.* **3,** 639–650
2. Offermanns, S. (2003) *Prog. Biophys. Mol. Biol.* **83,** 101–130
3. McCudden, C. R., Hains, M. D., Kimple, R. J., Siderovski, D. P., and Willard, F. S. (2005) *Cell Mol. Life Sci.* **62,** 551–577
4. Sunahara, R. K., and Taussig, R. (2002) *Mol. Interv.* **2,** 168–184
5. Fukuhara, S., Chikumi, H., and Gutkind, J. S. (2001) *Oncogene* **20,** 1661–1668
6. Rhee, S. G. (2001) *Annu. Rev. Biochem.* **70,** 281–312
7. Lutz, S., Shankaranarayanan, A., Coco, C., Ridilla, M., Nance, M. R., Vettel, C., Baltus, D., Evelyn, C. R., Neubig, R. R., Wieland, T., and Tesmer, J. J. (2007) *Science* **318,** 1923–1927
8. Tesmer, V. M., Kawano, T., Shankaranarayanan, A., Kozasa, T., and Tesmer, J. J. (2005) *Science* **310,** 1686–1690
9. Hollinger, S., and Hepler, J. R. (2002) *Pharmacol. Rev.* **54,** 527–559
10. Willard, M. D., Willard, F. S., and Siderovski, D. P. (2009) in *Handbook of*

Cell Signaling (Bradshaw, R., and Dennis, E., eds) 2nd Ed., Elsevier, San Diego, in press
11. Siderovski, D. P., Hessel, A., Chung, S., Mak, T. W., and Tyers, M. (1996) *Curr. Biol.* **6,** 211–212
12. Heximer, S. P., Knutsen, R. H., Sun, X., Kaltenbronn, K. M., Rhee, M. H., Peng, N., Oliveira-dos-Santos, A., Penninger, J. M., Muslin, A. J., Steinberg, T. H., Wyss, J. M., Mecham, R. P., and Blumer, K. J. (2003) *J. Clin. Invest.* **111,** 445–452
13. Tang, K. M., Wang, G. R., Lu, P., Karas, R. H., Aronovitz, M., Heximer, S. P., Kaltenbronn, K. M., Blumer, K. J., Siderovski, D. P., Zhu, Y., Mendelsohn, M. E., Tang, M., and Wang, G. (2003) *Nat. Med.* **9,** 1506–1512
14. Gu, S., Tirgari, S., and Heximer, S. P. (2008) *Mol. Pharmacol.* **73,** 1037–1043
15. Semplicini, A., Lenzini, L., Sartori, M., Papparella, I., Calò, L. A., Pagnin, E., Strapazzon, G., Benna, C., Costa, R., Avogaro, A., Ceolotto, G., and Pessina, A. C. (2006) *J. Hypertens.* **24,** 1115–1124
16. Oliveira-Dos-Santos, A. J., Matsumoto, G., Snow, B. E., Bai, D., Houston, F. P., Whishaw, I. Q., Mariathasan, S., Sasaki, T., Wakeham, A., Ohashi, P. S., Roder, J. C., Barnes, C. A., Siderovski, D. P., and Penninger, J. M. (2000) *Proc. Natl. Acad. Sci. U.S.A.* **97,** 12272–12277
17. Yalcin, B., Willis-Owen, S. A., Fullerton, J., Meesaq, A., Deacon, R. M., Rawlins, J. N., Copley, R. R., Morris, A. P., Flint, J., and Mott, R. (2004) *Nat. Genet.* **36,** 1197–1202
18. Cui, H., Nishiguchi, N., Ivleva, E., Yanagi, M., Fukutake, M., Nushida, H., Ueno, Y., Kitamura, N., Maeda, K., and Shirakawa, O. (2008) *Neuropsychopharmacology* **33,** 1537–1544
19. Smoller, J. W., Paulus, M. P., Fagerness, J. A., Purcell, S., Yamaki, L. H., Hirshfeld-Becker, D., Biederman, J., Rosenbaum, J. F., Gelernter, J., and Stein, M. B. (2008) *Arch. Gen. Psychiatry* **65,** 298–308
20. Soundararajan, M., Willard, F. S., Kimple, A. J., Turnbull, A. P., Ball, L. J., Schoch, G. A., Gileadi, C., Fedorov, O. Y., Dowler, E. F., Higman, V. A., Hutsell, S. Q., Sundström, M., Doyle, D. A., and Siderovski, D. P. (2008) *Proc. Natl. Acad. Sci. U.S.A.* **105,** 6457–6462
21. Heximer, S. P., Srinivasa, S. P., Bernstein, L. S., Bernard, J. L., Linder, M. E., Hepler, J. R., and Blumer, K. J. (1999) *J. Biol. Chem.* **274,** 34253–34259
22. Keys, J. R., Greene, E. A., Koch, W. J., and Eckhart, A. D. (2002) *Hypertension* **40,** 660–666
23. Takimoto, E., Koitabashi, N., Hsu, S., Ketner, E. A., Zhang, M., Nagayama, T., Bedja, D., Gabrielson, K. L., Blanton, R., Siderovski, D. P., Mendelsohn, M. E., and Kass, D. A. (2009) *J. Clin. Invest.* **119,** 408–420
24. Akhter, S. A., Luttrell, L. M., Rockman, H. A., Iaccarino, G., Lefkowitz, R. J., and Koch, W. J. (1998) *Science* **280,** 574–577
25. Wettschureck, N., Rütten, H., Zywietz, A., Gehring, D., Wilkie, T. M., Chen, J., Chien, K. R., and Offermanns, S. (2001) *Nat. Med.* **7,** 1236–1240
26. Kimple, A. J., Willard, F. S., Giguère, P. M., Johnston, C. A., Mocanu, V., and Siderovski, D. P. (2007) *Biochim. Biophys. Acta* **1774,** 1213–1220
27. Stols, L., Zhou, M., Eschenfeldt, W. H., Millard, C. S., Abdullah, J., Collart, F. R., Kim, Y., and Donnelly, M. I. (2007) *Protein Expr. Purif.* **53,** 396–403
28. Willard, F. S., Kimple, R. J., Kimple, A. J., Johnston, C. A., and Siderovski, D. P. (2004) *Methods Enzymol.* **389,** 56–71
29. Willard, F. S., Low, A. B., McCudden, C. R., and Siderovski, D. P. (2007) *Cell. Signal.* **19,** 428–438
30. Willard, F. S., and Siderovski, D. P. (2006) *Anal. Biochem.* **353,** 147–149
31. Leslie, A. G. (1999) *Acta Crystallogr. D Biol. Crystallogr.* **55,** 1696–1702
32. Evans, P. R. (1993) in *Proceedings of the CCP4 Study Weekend on Data Collection and Processing* (Sawyer, L., Issacs, N., and Burley, S., eds) pp. 114–122, Science and Engineering Research Council/Daresbury Laboratory, Warrington, England
33. Storoni, L. C., McCoy, A. J., and Read, R. J. (2004) *Acta Crystallogr. D Biol. Crystallogr.* **60,** 432–438
34. Murshudov, G. N., Vagin, A. A., and Dodson, E. J. (1997) *Acta Crystallogr. D Biol. Crystallogr.* **53,** 240–255
35. Emsley, P., and Cowtan, K. (2004) *Acta Crystallogr. D Biol. Crystallogr.* **60,** 2126–2132
36. Painter, J., and Merritt, E. A. (2006) *Acta Crystallogr. D Biol. Crystallogr.* **62,** 439–450
37. Sinnarajah, S., Dessauer, C. W., Srikumar, D., Chen, J., Yuen, J., Yilma, S., Dennis, J. C., Morrison, E. E., Vodyanoy, V., and Kehrl, J. H. (2001) *Nature* **409,** 1051–1055
38. Willard, F. S., Kimple, A. J., Johnston, C. A., and Siderovski, D. P. (2005) *Anal. Biochem.* **340,** 341–351
39. Popov, S., Yu, K., Kozasa, T., and Wilkie, T. M. (1997) *Proc. Natl. Acad. Sci. U.S.A.* **94,** 7216–7220
40. Wieland, T., Bahtijari, N., Zhou, X. B., Kleuss, C., and Simon, M. I. (2000) *J. Biol. Chem.* **275,** 28500–28506
41. Lan, K. L., Sarvazyan, N. A., Taussig, R., Mackenzie, R. G., DiBello, P. R., Dohlman, H. G., and Neubig, R. R. (1998) *J. Biol. Chem.* **273,** 12794–12797
42. Tesmer, J. J., Berman, D. M., Gilman, A. G., and Sprang, S. R. (1997) *Cell* **89,** 251–261
43. Druey, K. M., and Kehrl, J. H. (1997) *Proc. Natl. Acad. Sci. U.S.A.* **94,** 12851–12856
44. Srinivasa, S. P., Watson, N., Overton, M. C., and Blumer, K. J. (1998) *J. Biol. Chem.* **273,** 1529–1533
45. Slep, K. C., Kercher, M. A., Wieland, T., Chen, C. K., Simon, M. I., and Sigler, P. B. (2008) *Proc. Natl. Acad. Sci. U.S.A.* **105,** 6243–6248
46. Skiba, N. P., Yang, C. S., Huang, T., Bae, H., and Hamm, H. E. (1999) *J. Biol. Chem.* **274,** 8770–8778
47. Hepler, J. R., Berman, D. M., Gilman, A. G., and Kozasa, T. (1997) *Proc. Natl. Acad. Sci. U.S.A.* **94,** 428–432
48. Seack, J., Kruse, M., and Müller, W. E. (1998) *Biochim. Biophys. Acta* **1401,** 93–103
49. Suga, H., Koyanagi, M., Hoshiyama, D., Ono, K., Iwabe, N., Kuma, K., and Miyata, T. (1999) *J. Mol. Evol.* **48,** 646–653
50. Sierra, D. A., Gilbert, D. J., Householder, D., Grishin, N. V., Yu, K., Ukidwe, P., Barker, S. A., He, W., Wensel, T. G., Otero, G., Brown, G., Copeland, N. G., Jenkins, N. A., and Wilkie, T. M. (2002) *Genomics* **79,** 177–185
51. Chiba, S., Sasaki, A., Nakayama, A., Takamura, K., and Satoh, N. (2004) *Zool. Sci.* **21,** 285–298
52. Davidson, B. (2007) *Semin. Cell Dev. Biol.* **18,** 16–26
53. Pancer, Z., Mayer, W. E., Klein, J., and Cooper, M. D. (2004) *Proc. Natl. Acad. Sci. U.S.A.* **101,** 13273–13278
54. McKenzie, D. J., Farrell, A. P., and Brauner, C. J. (2007) *Primitive Fishes*, Academic Press, Amsterdam
55. Davison, I. G., Wright, G. M., and DeMont, M. E. (1995) *J. Exp. Biol.* **198,** 2185–2196
56. Evans, D. H., and Claiborne, J. B. (2006) *The Physiology of Fishes*, CRC, Taylor & Francis, Boca Raton, FL
57. Ingi, T., Krumins, A. M., Chidiac, P., Brothers, G. M., Chung, S., Snow, B. E., Barnes, C. A., Lanahan, A. A., Siderovski, D. P., Ross, E. M., Gilman, A. G., and Worley, P. F. (1998) *J. Neurosci.* **18,** 7178–7188
58. Cladman, W., and Chidiac, P. (2002) *Mol. Pharmacol.* **62,** 654–659
59. Hains, M. D., Siderovski, D. P., and Harden, T. K. (2004) *Methods Enzymol.* **389,** 71–88
60. Heximer, S. P., and Blumer, K. J. (2007) Sci. STKE **2007,** pe2
61. Notredame, C., Higgins, D. G., and Heringa, J. (2000) *J. Mol. Biol.* **302,** 205–217
62. Galtier, N., Gouy, M., and Gautier, C. (1996) *Comput. Appl. Biosci.* **12,** 543–548
63. Huelsenbeck, J. P., and Ronquist, F. (2001) *Bioinformatics* **17,** 754–755
64. Ronquist, F., and Huelsenbeck, J. P. (2003) *Bioinformatics* **19,** 1572–1574
65. Perrière, G., and Gouy, M. (1996) *Biochimie* **78,** 364–369